Holloway et al., http://www.jcb.org/cgi/content/full/jcb.201401122/DC1

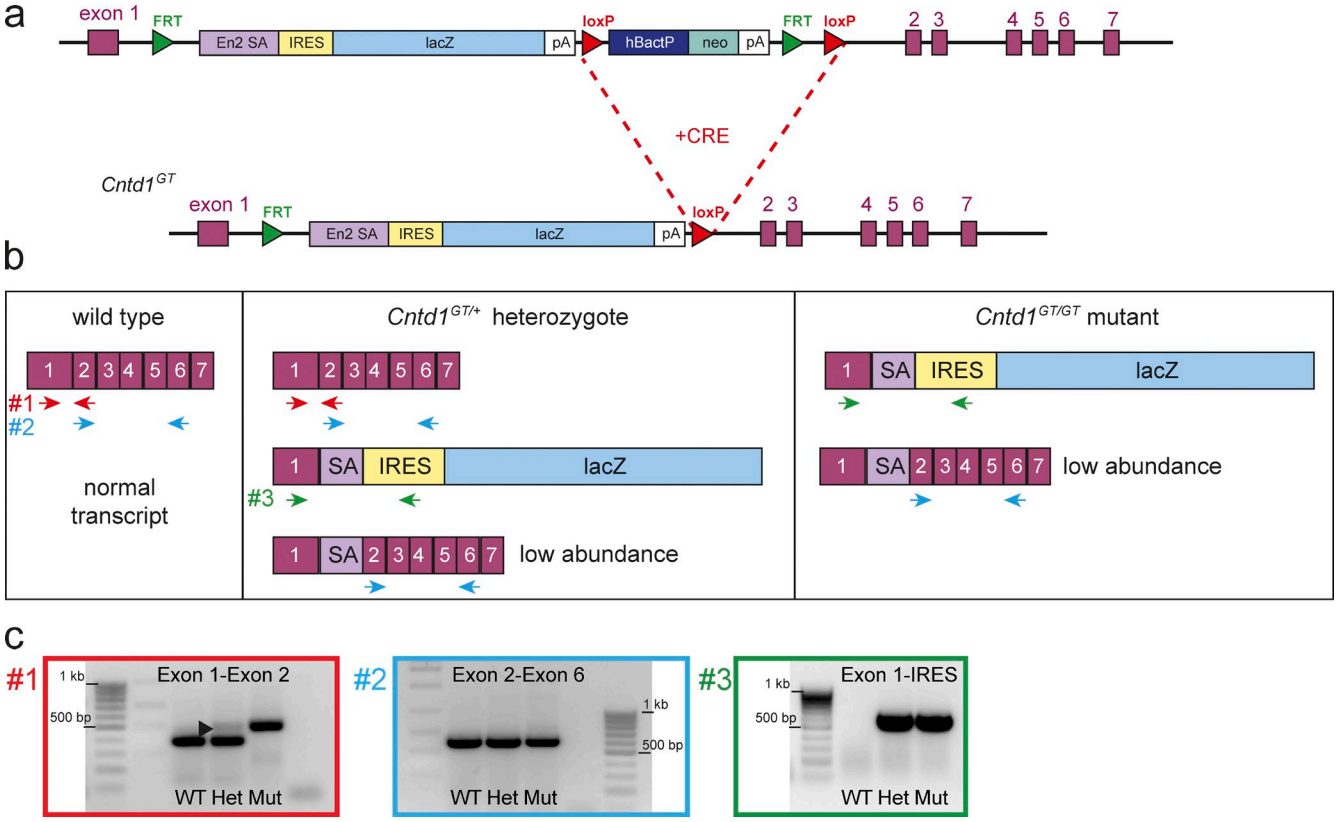


Figure S1. **The *Cntd1*$^{GT}$ allele severely reduces or eliminates *Cntd1* function.** (a) A gene trap embryonic stem cell line obtained from the Knockout Mouse Consortium (Knockout Mouse Project) was used to generate a targeted gene trap mouse line. CRE-mediated excision of the *neo* cassette was achieved by crossing mice bearing the initial targeted allele (top) to a *Spo11-Cre* mouse line (Lyndaker et al., 2013) followed by breeding the *neo*-excised progeny through several generations to achieve a fully *neo*-excised genetrap allele (bottom) that we have named *Cntd1*$^{GT}$. (b) Structures of transcripts expressed from the *Cntd1* locus in WT, *Cntd1*$^{GT/+}$ heterozygous, and *Cntd1*$^{GT/GT}$ homozygous mutant testes, deduced from RT-PCR analyses (some shown in c), quantitative PCR (not depicted), and expression of LacZ protein (not depicted). WT animals only express the normal transcript, comprising exons 1–7. In *Cntd1*$^{GT/+}$ heterozygotes and *Cntd1*$^{GT/GT}$ homozygotes, in addition to producing the expected major transcript encoding exon 1–LacZ, the *Cntd1*$^{GT}$ allele also produces a minor transcript in low abundance, in which a cryptic splice donor near the end of exon 1 is spliced to a cryptic exon comprising a portion of the vector-derived splice acceptor cassette (SA), which is in turn spliced to exon 2; this minor transcript encodes a predicted protein with a 37–amino acid sequence inserted into the middle of α helix #1 of the N-terminal cyclin box of CNTD1. Because the N-terminal cyclin box is highly constrained structurally, this insertion is predicted to severely disrupt protein structure, stability, and function. Colored arrows indicate primer pairs used to detect different transcript species in the RT-PCR analysis depicted in c. (c) Example RT-PCR analyses used to deduce the structures of the transcripts produced by the *Cntd1*$^{GT}$ allele. For each gel, RT-PCR was performed using RNA extracted from wild-type (WT), *Cntd1*$^{GT/+}$ heterozygote (Het), or *Cntd1*$^{GT/GT}$ mutant (Mut) testes. Box 1 shows that no WT transcripts are detected in *Cntd1*$^{GT/GT}$ homozygotes; only the insert-containing transcripts are detected using the exon 1–exon 2 primer pair. The arrowhead shows the larger PCR product of the mutant allele. IRES, internal ribosome entry site.

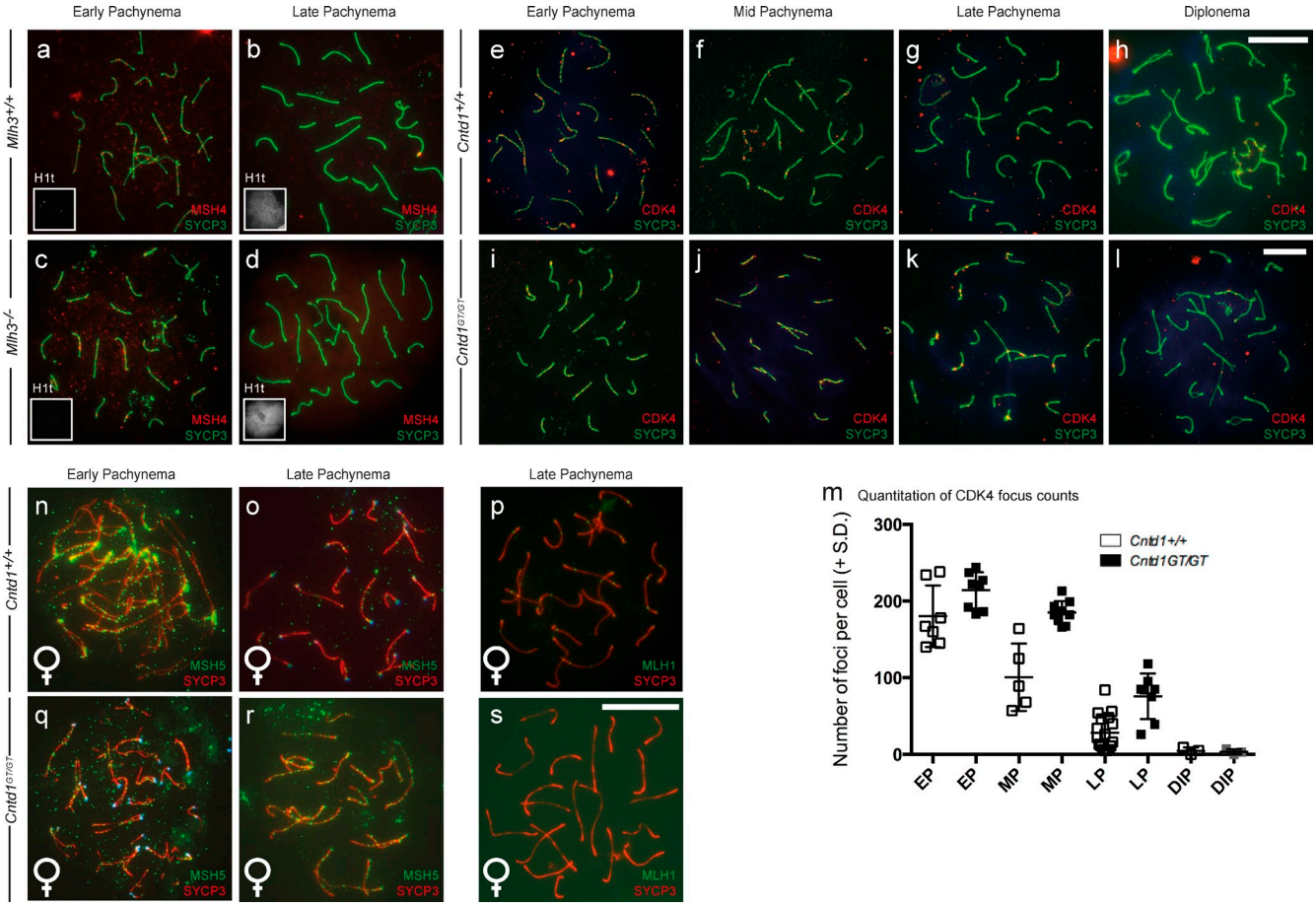


Figure S2. **Accumulation of meiotic markers in *Mlh3*$^{-/-}$ spermatocytes, *Cntd1*$^{GT/GT}$ spermatocytes, and *Cntd1*$^{GT/GT}$ oocytes.** (a–d) MSH4 staining in pachytene spermatocytes from *Mlh3*$^{-/-}$ mice. Early (a and c) and late (b and d) pachytene spermatocytes from WT (a and b) and *Mlh3* mutant (c and d) mice, stained with antibodies against SYCP3 and MSH4. Insets show H1t staining (as a staging indicator for mid- to late pachynema) for the corresponding cells. In spermatocytes from both WT and *Mlh3*$^{-/-}$ males, MSH4 foci associated with chromosome cores were abundant in early pachynema but absent by late pachynema. (e–m) Localization of CDK4 on meiotic chromosome cores during prophase I. Chromosome spreads from early pachytene through diplotene stage spermatocytes from *Cntd1*$^{+/+}$ (e–h) and *Cntd1*$^{GT/GT}$ (i–l) males, simultaneously stained for CDK4 and SYCP3. Panel m shows the quantitation of CDK4 foci in WT and *Cntd1*$^{GT/GT}$ males (means ± SD). EP, early pachynema; MP, midpachynema; LP, late pachynema; DIP, diplonema. Mann–Whitney *U* tests were performed to show statistically significant differences between WT and mutant CDK4 counts at midpachynema ($P < 0.001$) and late pachynema ($P < 0.0001$). (n–s) Meiotic marker localization during pachynema in oocytes from *Cntd1*$^{+/+}$ (n–p) and *Cntd1*$^{GT/GT}$ (q–s) females, stained with antibodies against SYCP3 and either MSH5 (n, o, q, and r) or MLH1 (p and s). Bars, 10 µm (bar in s applies to n–s).

**a**

>HEI10 (CCNB1IP1)

MSLCEDMLLCNYRKCRIKLSGYAWVTACSHIFCDQHGSGEFSRSPAICPACNSTLSGKLDIVRTELSPSE
EYKAMV**LAGLRPEVVLDISSRALAFWTYQV**HQERLYQEYNFSKAENHLKQMEKMYMQQIQSKNIELTSMK
GEVISMKKVLEEYKKKFSDISEKLMERNRQYQKLQGLYDSLRLRNITIASQEGSLEPGMIPQSGVFGFPP
GNNSKFSLDHIPVGNQGGGDEDVQFRPFFVCSPTAPEPINNFFSFASPSHEAEQQVCSRAFKAKRI

**b**

>RNF212

MASWVFCNRCFQSPHRKSSFSLTSCGHVYCHSCLLKGTKNECVICQAPCQTVLLSKHTNSNIQTFFLGID
GLCKKYSQETSQISEFQEKHRRRLVAFYQEKISQLEESLRKSVLQIKQLQSMRSSQQPAFNKIKNSVSSK
PNGYLFLPPNSSLPDRIESMDIDLTPPARKPEMSAGPSRISVISPPQDGRMG*SVTCRGPQHLSLTPSHAS*
*MTKASRVPPLQMPYKELSPPPASQLSSRATQGPSPSVSSSWTGPPRQPISISGLLQRQCAGSASPRGMDT*
*EKMSPFLPSTPTNLRSVASPWHACVHR*

**c**

>MutSγ subunit MSH4

MCCLFLRLRDYSTAHALSLPPCQRCGLQPWSARSHARRTLGVRKAGEMLRQEAASLSSSPRWTPSRRDAP
CGRTLASASRPSTEGAMADRSSSSSSSPAPASAPGSSFGNKRSYAIHRAASSFPVGTSSSSARDTTYPHT
FRTPLSAGNPQRSGHKSWTPQVGYSATSSAVSAHAPSVIVAVVEGRGLARGEIGMASIDLKSPQIMLSQF
ADNTTYAKVITKLQVLSPLEIIMSNTACVVGNSTKLFTLITENFKNVNFTTVQRKYFNETKGLEYIEQLC
IAEFSSVLMEVQSRYYCLAAAAAALLKYVEFIQNSVYAPKSLKIYFQGSEQTAMIDSSSAQNLELLVNNQD
YRSNHTLFGVLNYTKTAGGSRRLRSNILEPLVDVETISMRLDCVQELLQDEELFFGLQSVISRFLDTEQL
LSVLVQIPKQDTVNAAESKITNLIYLKHTLELVEPLKVTLKNCSTPLLRAYYGSLEDHRFGLILDKIKTV
INDDARYMKGCLNMRTQKCYAVRSNISEFLDIARRTYTEIVDDIAGMIAQLAEKYSLPLRTSFSSSRGFF
IQMTTDCAALSSDQLPSEFIKISKVKNSYSFTSADLIKMNERCQESLREIYHMTYMIVCKLLSEIYEHIH
CLYKLSDTVSMLDMLLSFAHACTLSDYVRPEFTDTLAIKQGWHPILEKISAEKPVANNTYITEGSNVLII
TGPNMSGKSTYLKQIALCQIMAQIGSYVPAEYASFRIAAQIFTRISTDDDIETNSSTFMKEMKEIAYILH
NANDKSLILIDELGRGTNTEEGIGISYAVCEHLLSIKAFTLFTTHFLELCHLDALYLNVENMHFEVQHVK
NTSRNKDAILYTYKLSRGLTEEKNYGLKAAEASSLPSSIVLDARDITTQITRQILQNQRSSPEMDRQRAV
YHLATRLVQAARNSQLEPDRLRTYLSNLKKKYAGDFPRAVGLPEKTEE

> MutSγ subunit MSH5

MAFRATPGRTPPGPGPRSGIPSASFPSPQPPMAGPGGIEEEDEEEPAEIHLCVLWSSGYLGIAYYDTSDS
TIHFMPDAPDHESLKLLQRVLDEINPQSVVTSAKQDEAMTRFLGKLASEEHREPKGPEIILLPSVDFGPE
ISKQRLLSGNYSFISDSMTATEKILFLSSIIPFDCVLTVRALGGLLKFLSRRRIGVELEDYDVGVPILGF
KKFVLTHLVSIDQDTYSVLQIFKSESHPSVYKVASGLKEGLSLFGILNRCRCKWGQKLLRLWFTRPTREL
RELNSRLDVIQFFLMPQNLDMAQMLHRLLSHIKNVPLILKRMKLSHTKVSDWQVLYKTVYSALGLRDACR
SLPQSIQLFQDIAQEFSDDLHHIASLIGKVVDFEESLAENRFTVLPNIDPDIDAKKRRLIGLPSFLTEVA
QKELENLDSRIPSCSVIYIPLIGFLLSIPRLPFMVEASDFEIEGLDFMFLSEDKLHYRSARTKELDTLLG
DLHCEIRDQETLLMYQLQCQVLARASVLTRVLDLASRLDVLLALASAARDYGYSRPHYSPCIHGVRIRNG
RHPLMELCARTFVPNSTDCGGDQGRVKVITGPNSSGKSIYLKQVGLITFMALVGSFVPAEEAEIGVIDAI
FTRIHSCESISLGLSTFMIDLNQVAKAVNNATEHSLVLIDEFGKGTNSVDGLALLAAVLRHWLALGPSCP
HVFVATNFLSLVQLQLLPQGPLVQYLTMETCEDGEDLVFFYQLCQGVASASHASHTAAQAGLPDPLIARG
KEVSDLIRSGKPIKATNELLRRNQMENCQALVDKFLKLDLEDPTLDLDIFISQEVLPAAPTIL

Figure S3. **Predicted cyclin-binding motifs and CDK phosphorylation sites in HEI10, RNF212, and MutSγ.** (a–c) Sequences of the indicated proteins, with predicted cyclin-binding RXL motifs highlighted in magenta and potential CDK phosphorylation sites [S/T]P highlighted in green. In a, blue highlighting indicates the amino acid segment (including the RXL motif) that is absent in the mutant HEI10 protein encoded by the *Hei10*$^{mei4}$ allele. Yellow highlighting indicates the portions of the proteins that are conserved among diverse animals and plants (a and c) or among diverse animals (b); gray indicates regions that are poorly conserved or nonconserved. Note that in RNF212, MSH4, and MSH5, the majority of [S/T]P sites are located in nonconserved N- or C-terminal tails. In b, the gray sequence is italicized and underlined to indicate that this region of RNF212 is highly diverged even within mammals.

## Reference

Lyndaker, A.M., P.X. Lim, J.M. Mleczko, C.E. Diggins, J.K. Holloway, R.J. Holmes, R. Kan, D.H. Schlafer, R. Freire, P.E. Cohen, and R.S. Weiss. 2013. Conditional inactivation of the DNA damage response gene Hus1 in mouse testis reveals separable roles for components of the RAD9-RAD1-HUS1 complex in meiotic chromosome maintenance. *PLoS Genet.* 9:e1003320. http://dx.doi.org/10.1371/journal.pgen.1003320